CHAPTER 14

TERNARY FOUR-PHASE EQUILIBRIUM—CLASS I

Ternary eutectic reaction occurs by the "isothermal" decomposition of liquid into three different solid phases:

$$L \underset{\text{heating}}{\overset{\text{cooling}}{\rightleftharpoons}} \alpha + \beta + \gamma$$

This is known also as *four-phase equilibrium of the first kind* or as an example of *class I four-phase equilibrium.* It is represented in the space model by a unique tie-triangle, the ternary eutectic isotherm (or plane), which connects the compositions of the four phases participating in the reaction at the ternary eutectic temperature (Fig. 14-1). In this diagram the ternary eutectic plane has been shaded to make its location more apparent. The three corners of the triangle touch the three one-phase regions α, β, and γ and are so labeled. The liquid composition occurs at point L within the triangle, where the liquidus surfaces from the three corners of the space diagram meet at the lowest melting point of the ternary system.

According to the phase rule, four-phase equilibrium in ternary systems should be univariant:

$$P + F = C + 2$$
$$4 + 1 = 3 + 2$$

Having established the pressure, the temperature of four-phase equilibrium and the compositions of each of the four phases should be fixed. The construction employed in Fig. 14-1 meets these requirements; the ternary eutectic plane is isothermal, and the compositions of the four phases are designated at four fixed points on the eutectic plane.

A fuller understanding of the internal structure of the ternary eutectic diagram may be had by reference to the "exploded model" in Fig. 14-2. The diagram is qualitatively symmetrical with respect to each of its three corners or three sides, there being only six different kinds of fields, of which all except the ternary eutectic plane have been encountered in previous chapters.

Three three-phase fields $L + \alpha + \beta$, $L + \alpha + \gamma$, and $L + \beta + \gamma$, Fig. 14-2, emerge downward from the three corresponding binary eutectic

reactions, Fig. 14-1, and terminate upon the ternary eutectic plane $L + \alpha + \beta + \gamma$. The bottom tie-triangle in each of these fields joins those in the other two three-phase fields to form one larger tie-triangle, the ternary eutectic plane. Thus triangle 1-5-3 of the $L + \alpha + \beta$ field, triangle 1-2-4 of the $L + \alpha + \gamma$ field, and triangle 2-3-6 of the $L + \beta + \gamma$ field join to form triangle 4-5-6 of the ternary eutectic plane. Below the ternary eutectic temperature the three-phase field $\alpha + \beta + \gamma$ begins with the tie-triangle 4-5-6 and descends in a series of tie-triangles to the base of the space diagram.

Surmounting the three-phase fields are three two-phase fields $L + \alpha$, $L + \beta$, and $L + \gamma$. These are bounded by liquidus and solidus surfaces connected at all points by tie-lines joining the conjugate liquid and solid compositions. Each is wedge-shaped on its underside, having two ruled surfaces which are, respectively, identical with one top surface on each of two three-phase fields. For example, the region $L + \beta$ has an undersurface 12-9-3-17 composed of tie-lines joining the conjugate liquid and β phases along the lines 9 and 17, respectively, and being identical with the surface 12-9-3-17 on the $L + \beta + \gamma$ field. Its other lower surface is 3-8-11-16, which coincides with the surface of like designation on the $L + \alpha + \beta$ field. Line 3, it will be noted, lies in the ternary eutectic plane and connects the liquid composition at the eutectic point with the β of the ternary eutectic. Similar relationships will be observed upon the $L + \alpha$ and $L + \gamma$ fields.

There are also three two-phase fields representing the coexistence of three pairs of solid phases: $\alpha + \beta$, $\alpha + \gamma$, and $\beta + \gamma$. These are slablike fields bounded on their vertical ends by solvus surfaces between which run tie-lines connecting pairs of conjugate solid phases. Upon the $\alpha + \beta$ field, Fig. 14-2, for example, the solvus surfaces are 26-15-23 and 24-16-31. The upper surface of this field 5-15-11-16 is a ruled surface composed of tie-lines joining compositions of α along line 15 with compositions of β along line 16; this surface is identical with the ruled undersurface of the L + α + β field 5-15-11-16. Another ruled surface 34-23-5-24 forms the front face of the $\alpha + \beta$ region, again being composed of tie-lines connecting α and β compositions along the lines 23 and 24 and coincident with the rear side of the $\alpha + \beta + \gamma$ field. These constructions are duplicated in the $\alpha + \gamma$ and $\beta + \gamma$ fields.

One-phase regions fill the remaining space of the ternary diagram. Above the three segments of the liquidus surface and extending down to the ternary eutectic point lies the region of liquid. At each corner of the space diagram is a one-phase field representing one of the three crystalline phases. These are represented in Fig. 14-2 and require no special comment except to point out that there is one corner on each (labeled α, β, and γ on the respective fields) which touches the ternary eutectic plane

and there are upon each one-phase field three edges (lines 14, 15, and 23 on the α field) which coincide with edges on three of the three-phase fields.

Viewed through the medium of isothermal sections, the essential simplicity of the ternary eutectic diagram is even more apparent. The seven isotherms of Fig. 14-3 are taken at the temperatures designated T_1 to T_7 in Fig. 14-1. In the first section T_1 the liquidus and solidus adjacent

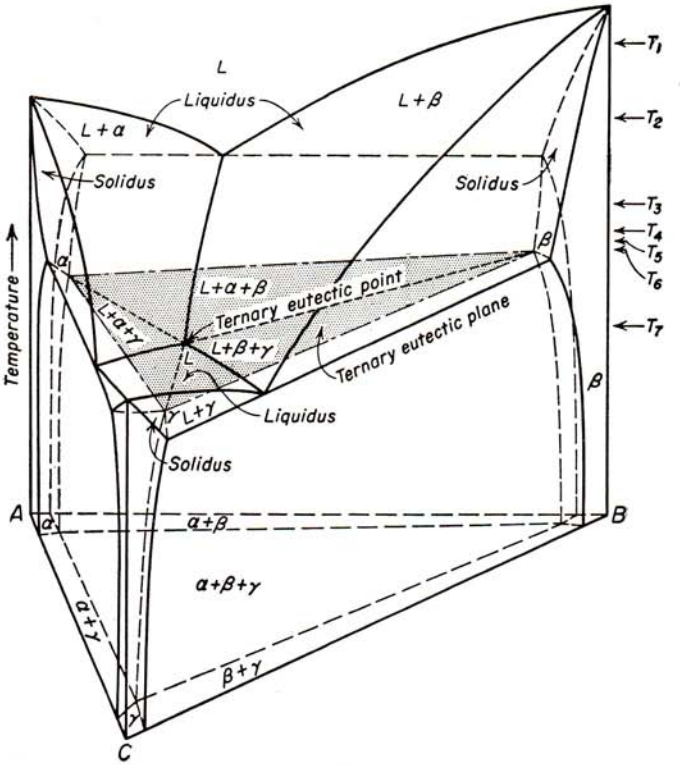

FIG. 14-1. Temperature-composition space diagram of a ternary eutectic system, illustrating class I four-phase equilibrium.

to B, the highest melting component, are intersected, revealing fields of L, β, and $L + \beta$. Successively at T_2 and T_3 the liquidus and solidus pairs adjacent to the A and C components are intersected. The third section T_3 is taken just below the eutectic temperature of the binary system AB and intersects the three-phase region $L + \alpha + \beta$ that originates upon the binary eutectic line. Similar constructions were found in each of the phase diagrams of the preceding chapter; for example, compare with section T_2 in Fig. 13-6. From each of the binary eutectic lines there issues a three-phase field so that at T_4, just below the binary eutectic of the

system AC, the field $L + \alpha + \gamma$ appears and at T_5, just below the BC eutectic, the $L + \beta + \gamma$ field appears. The liquid region is now confined to a small three-cornered area in the middle of the diagram, and the liquid plus solid regions have grown narrow. As the temperature falls, these fields continue to shrink, permitting the three three-phase tie-triangles to meet and to form the ternary eutectic plane at T_6, the ternary eutectic temperature. At this temperature the liquid phase disappears and with it the six other fields involving liquid, so that below the ternary eutectic temperature, only solid phases remain. As the extent of solid solubility decreases with falling temperature T_7, the $\alpha + \beta + \gamma$ field grows larger while the one-phase fields contract.

Vertical Sections

Vertical sections through the ternary eutectic diagram produce a wide variety of forms. The ternary eutectic plane appears only as a horizontal line in such sections; otherwise there is little regularity. Section XB of Fig. 14-4 has been so selected that it intersects the B corner of the space diagram and the ternary eutectic point. There are no tie-lines in this section, and all boundaries are curved, except the trace of the ternary eutectic plane. The next section, YZ, Fig. 14-5, has been caused to include

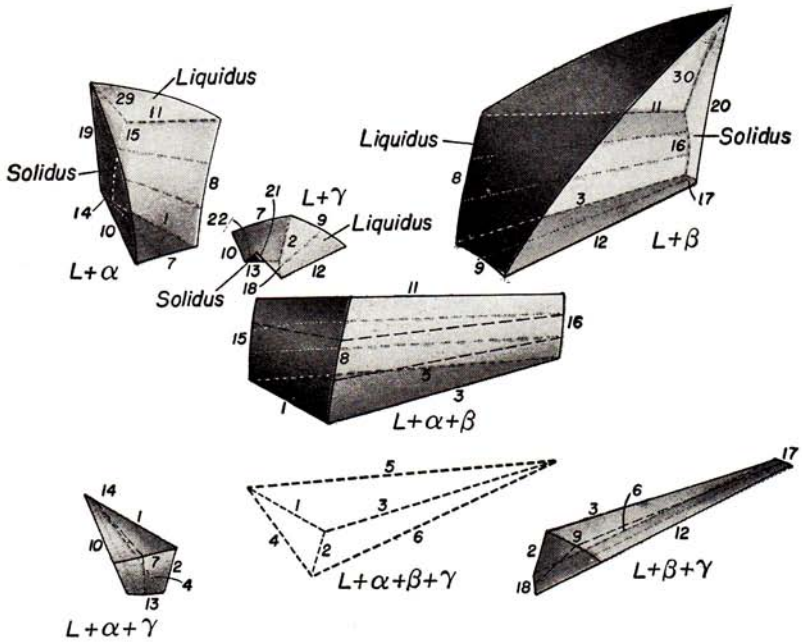

FIG. 14-2. Exploded model of the diagram of Fig. 14-1. The inscribed numbers

that line in the ternary eutectic plane which joins the composition of the liquid phase with that of the β, that is, the lowest tie-line of the $L + \beta$ field. Here the $L + \alpha + \beta$ field is not intersected and the $L + \beta$ field ends on the ternary eutectic line. Two sections parallel to the AB side of the space model are shown in Figs. 14-6 and 14-7; neither passes through the ternary eutectic point. It will be noted that whereas the three-phase regions are most often enclosed by three boundaries in Fig. 14-6, the $L + \alpha + \gamma$ and $L + \beta + \gamma$ fields are enclosed by four boundaries each in Fig. 14-7. No tie-lines appear in either of these sections. As in previous examples, temperatures of transformation can be read from these vertical sections, but the compositions of the participating phases are shown

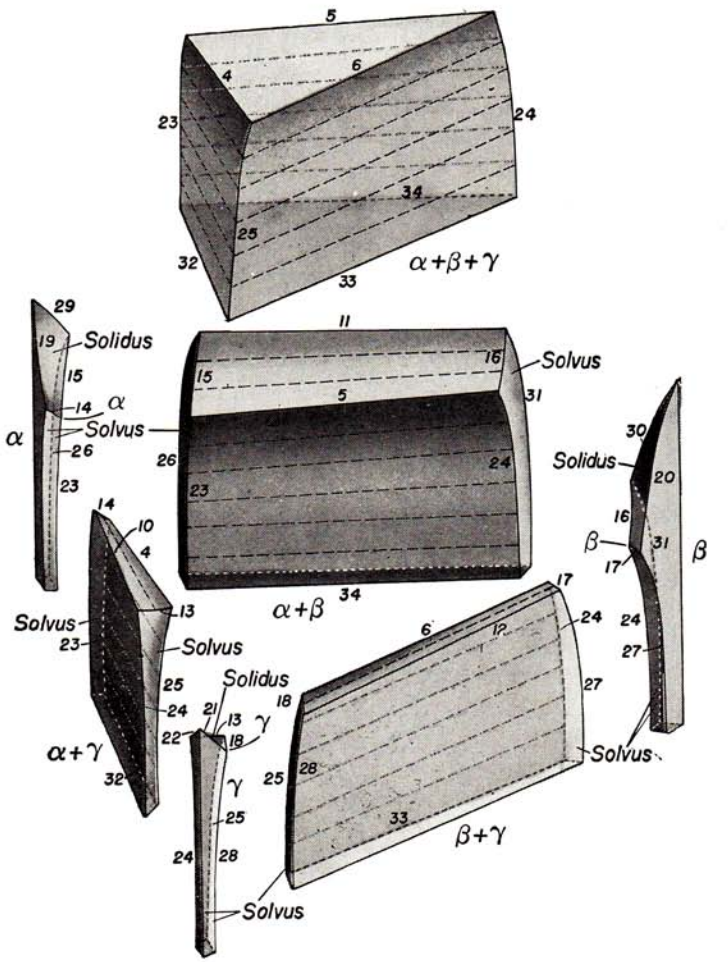

identify edges that are identical lines on different segments of the model.

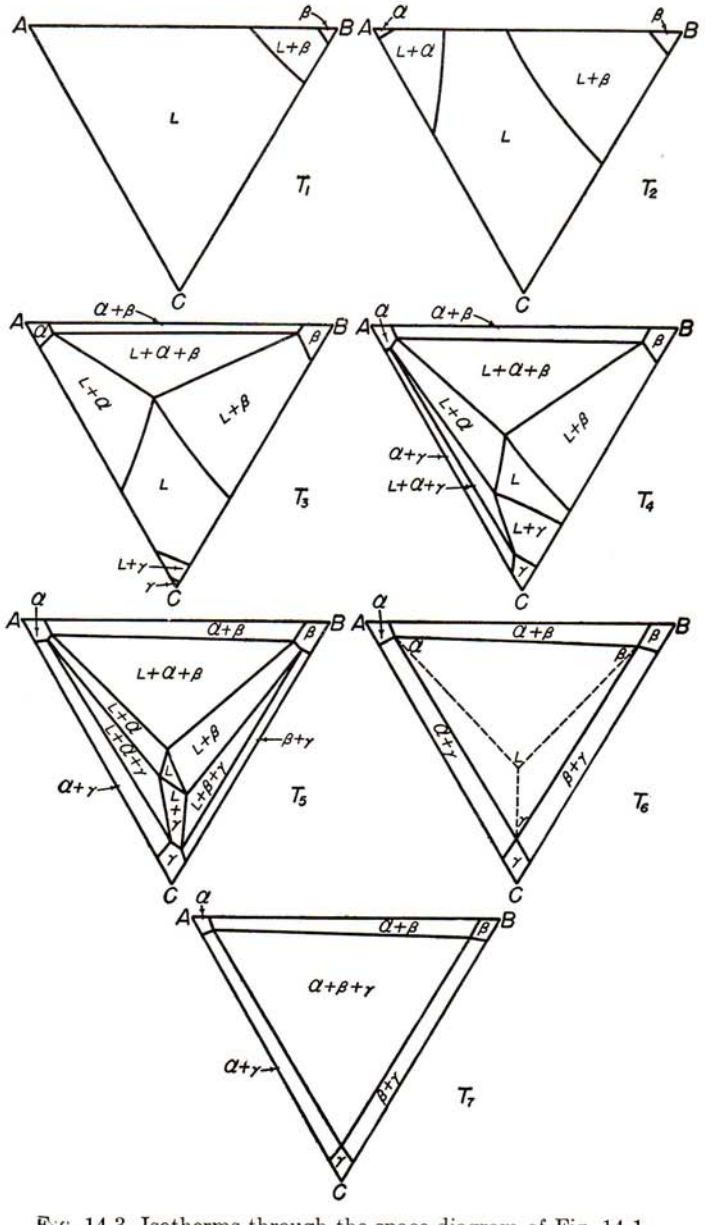

FIG. 14-3. Isotherms through the space diagram of Fig. 14-1.

only at a few specific points such as L and β at the ternary eutectic temperature in Fig. 14-5.

Freezing of the Ternary Eutectic Alloy

The alloy of lowest melting point, the *ternary eutectic alloy* (point L in isotherm T_6 of Fig. 14-3), freezes isothermally. Above the eutectic temperature, this alloy is fully molten, and below, it is entirely solid. At the

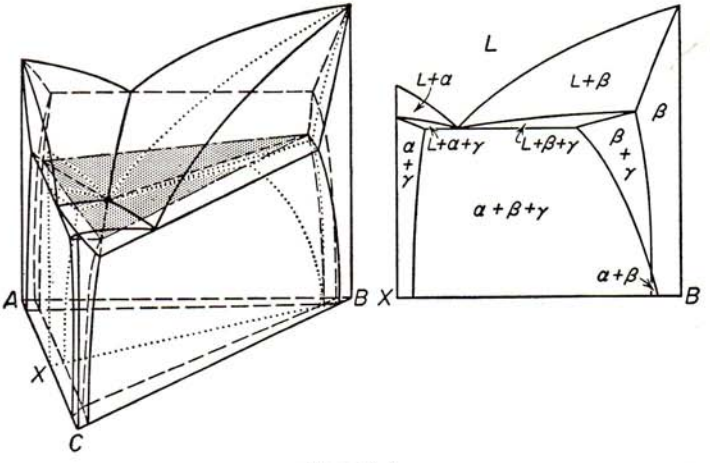

FIG. 14-4

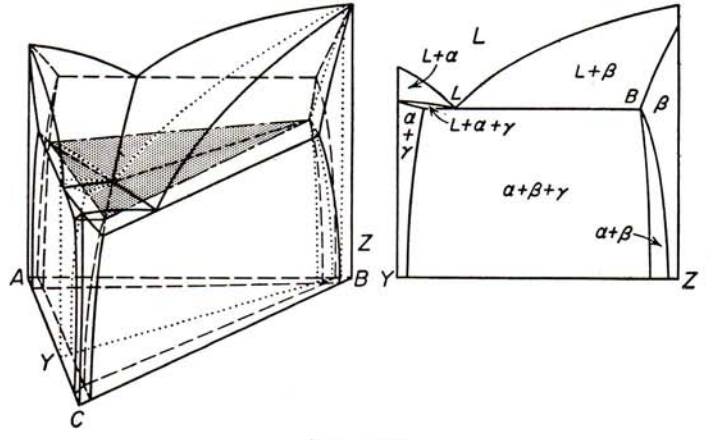

FIG. 14-5

eutectic temperature the liquid decomposes simultaneously into crystals of α, β, and γ. This process results in a fairly uniform distribution of the three solid phases in the microstructure of the alloy. An example of a ternary eutectic structure is given in Fig. 14-8A, which represents an

alloy composed of lead plus 11% antimony and 4% tin, composition e in Fig. 14-9. The lead-rich δ phase (medium gray), being present in major quantity in this eutectic, forms a matrix in which the antimony-rich α needles (white) and the β needles (black) are embedded. Since δ is the

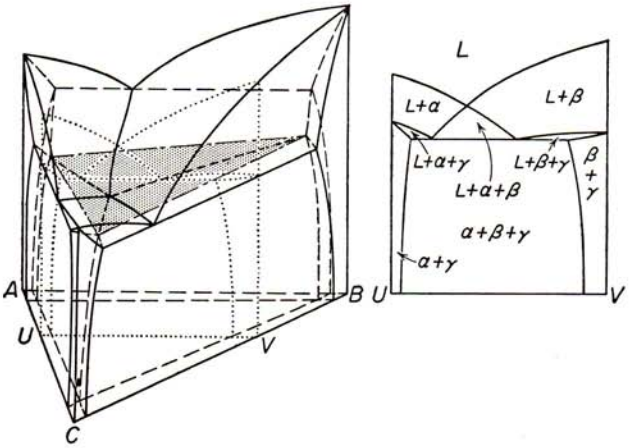

FIG. 14-6

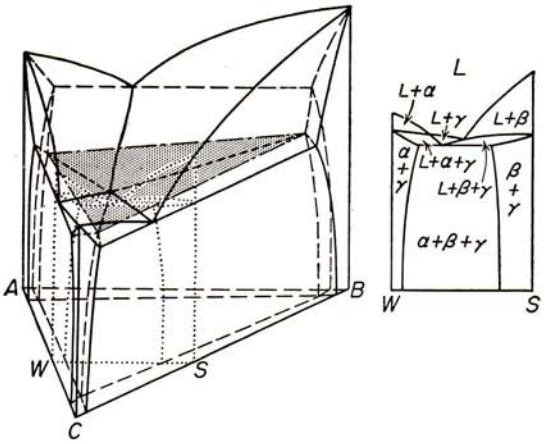

FIG. 14-7

continuous phase, the physical properties of this alloy more closely resemble those of the lead-rich phase than those of either of the other two phases.

Freezing of Other Alloys of the Ternary Eutectic System

When the gross composition departs from that of the eutectic, the freezing process may result in microstructures which exhibit (1) a one-

phase primary constituent with a two-phase secondary constituent and a three-phase tertiary constituent, alloy X in Fig. 14-9; (2) a two-phase primary constituent with a three-phase secondary constituent, alloy Y in Fig. 14-9; or (3) a one-phase primary constituent with a three-phase secondary constituent, alloy Z in Fig. 14-9. Photomicrographs of cast lead-tin-antimony alloys of these types are given in Fig. 14-8C, B, and D respectively.

Alloy X of Fig. 14-9 begins to freeze at 250°C when primary (idiomorphic) particles of the β phase (black) begin to separate (Fig. 14-8C). Just above 240°C this alloy enters the $L + \beta + \delta$ field and somewhat acicular particles of β crystallize, together with the δ phase (gray), in a Chinese script form that surrounds the primary β particles. All the liquid that remains at 240°C freezes isothermally to the ternary eutectic of $\alpha + \beta + \delta$.

This freezing process may be followed in a simplified manner by reference to a liquidus projection such as that shown in Fig. 14-10. Here the valleys of the liquidus surface are represented in solid lines, the outline of the ternary eutectic plane is dashed, and the other boundaries of the three-phase regions at the eutectic temperature are shown in dotted lines. Arrows proceeding from X toward e indicate the path of change of the liquid composition. At first, the liquid composition moves almost directly away from the B corner; during this stage the primary β phase is crystallizing. When the composition of the liquid reaches the valley that descends from the AB eutectic to the ternary eutectic, it follows this path, α and β crystallizing together meanwhile. At e, any remaining liquid freezes to a eutectic constituent without further change of composition.

Alloy Y lies upon the valley that descends from the $\beta\delta$ eutectic to the ternary eutectic point in Fig. 14-9. Consequently, freezing begins with the coseparation of two solid phases, β and δ (black needles in a gray matrix) in Fig. 14-8B. All liquid that remains at the ternary eutectic temperature, of course, freezes to a three-phase $\alpha + \beta + \delta$ eutectic structure. With equilibrium freezing no liquid would remain at the eutectic temperature, because composition Y lies outside the eutectic triangle, but with natural freezing the coring process will result in the extension of the freezing range and some liquid will be left when the ternary eutectic temperature is reached. In Fig. 14-10 it can be seen that the liquid composition travels directly down the liquidus valley from Y to e.

Alloy Z represents a special case in which the composition lies exactly on the line connecting the δ corner of the ternary eutectic triangle with the eutectic point. This line is also the lowest tie-line in the $L + \delta$ region and the line upon which the $L + \beta + \delta$ and $L + \alpha + \delta$ regions meet. Freezing begins with a primary separation of the δ phase, Fig. 14-8D, while the liquid composition moves directly toward the ternary eutectic

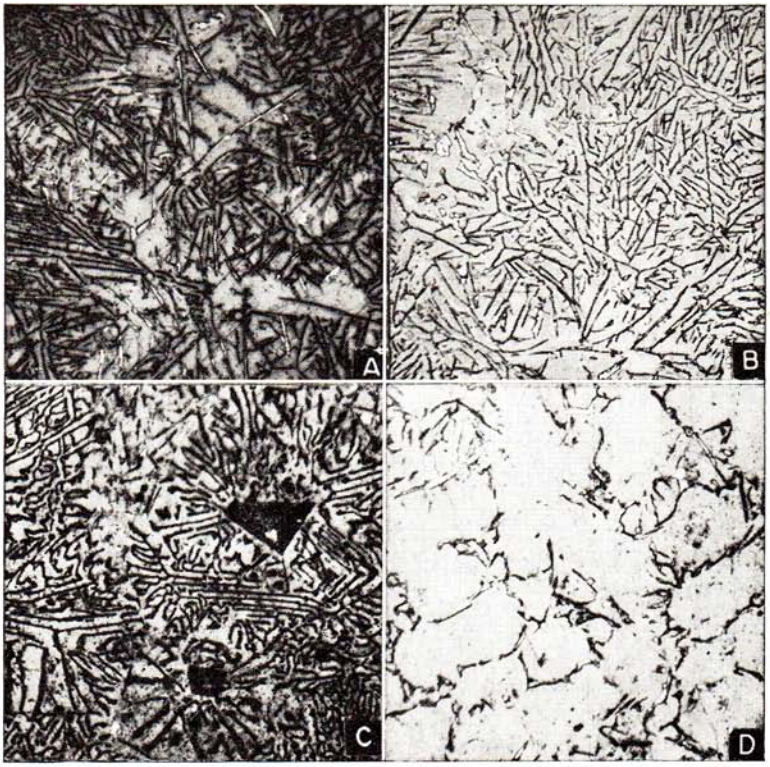

FIG. 14-8. Microstructure of four alloys of the lead-tin-antimony system in the as-cast state. The ternary eutectic alloy, shown at A (point e in Figs. 14-9 and 14-10), is composed of a light-colored matrix of δ supporting a large number of black β particles and a few white α particles; at B is shown an alloy the composition of which lies upon one of the liquidus valleys adjacent to the ternary eutectic (point Y in Figs. 14-9 and 14-10), so that primary freezing results in a two-phase crystallization of δ (light matrix) and β (black needles) followed by a secondary crystallization of the ternary eutectic. Shown at C, an alloy of random composition (point X in Figs. 14-9 and 14-10) freezes by the primary crystallization of large idiomorphic particles of β (black), a secondary separation of β (black needles) + α (white particles), and a tertiary freezing of the residual liquid as a ternary eutectic. Alloy D lies upon the line connecting the δ corner of the ternary eutectic plane with the eutectic liquid (point Z in Figs. 14-9 and 14-10) and is composed of primary δ dendrites interspersed with ternary eutectic. Magnification 50.

point e in Fig. 14-10. No valley of the liquidus is intersected, and no two-phase crystallization occurs. All remaining liquid is of ternary eutectic composition and freezes to the ternary eutectic constituent.

Thus, in place of the two basic types of microstructure of binary eutectic systems (the eutectic and the hypo- or hypereutectic), there are four distinct kinds of microstructure that are characteristic of ternary eutectic systems. None of these except the ternary eutectic itself is named. Under-

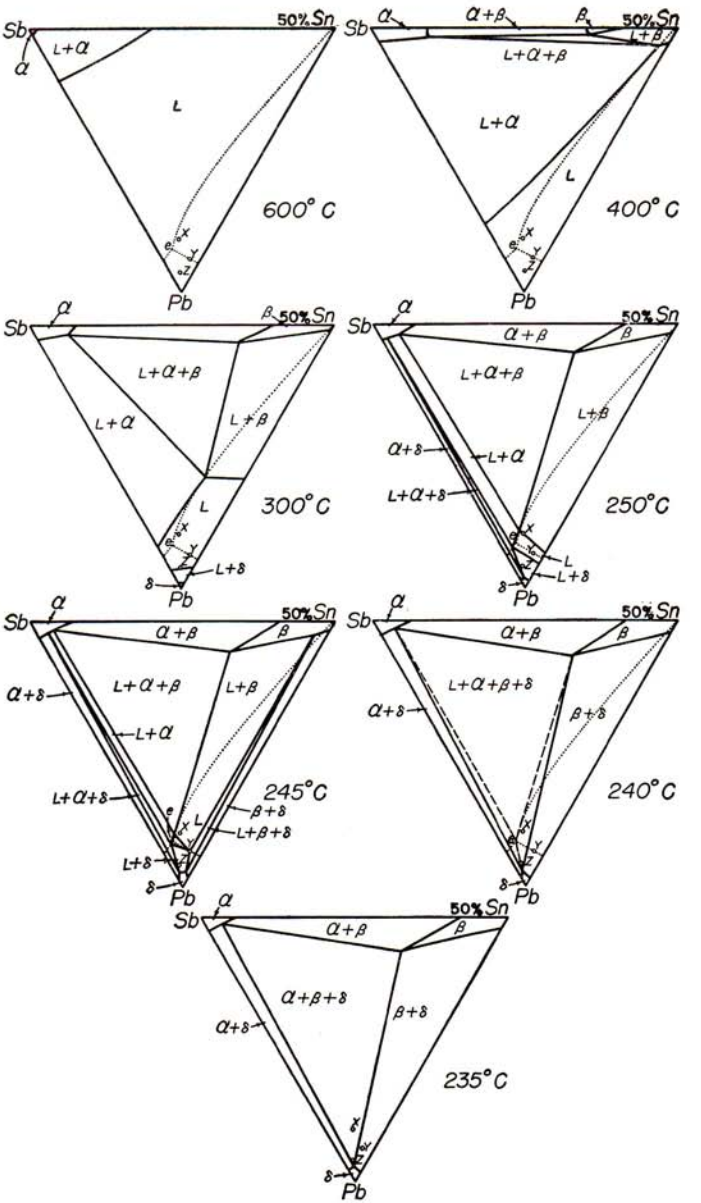

FIG 14-9. Isotherms from the ternary eutectic system Pb-Sb-β (50% Sb + 50% Sn). The letters e, X, Y, and Z indicate the compositions of the four alloys, the microstructure of which is shown in Fig. 14-8.

cooling is common in the freezing of ternary alloys, and as a consequence, the expected structures are often considerably modified. Also, divorcement of two-phase and three-phase constituents can lead to extensive alteration of the microstructure. This situation is further complicated by the fact that the binary three-phase reactions need not be of the eutectic types, but one or more may be peritectic type. The $L + \alpha + \beta$ equilibrium of the antimony-tin binary system is, in fact, of the peritectic type.

Heat Treatment

No new principles are involved in the heat treatment of alloys of ternary eutectic systems. Holding at temperature sufficiently high to accelerate diffusion causes the alloys to approach their equilibrium states. The end point of any such homogenization treatment can be read from the isothermal section

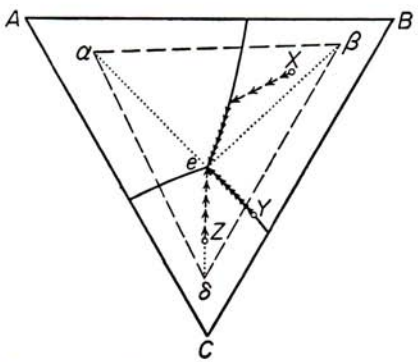

FIG. 14-10. Diagram showing by arrows the progress of composition change of the liquid phase during the freezing of alloys *X*, *Y*, and *Z*.

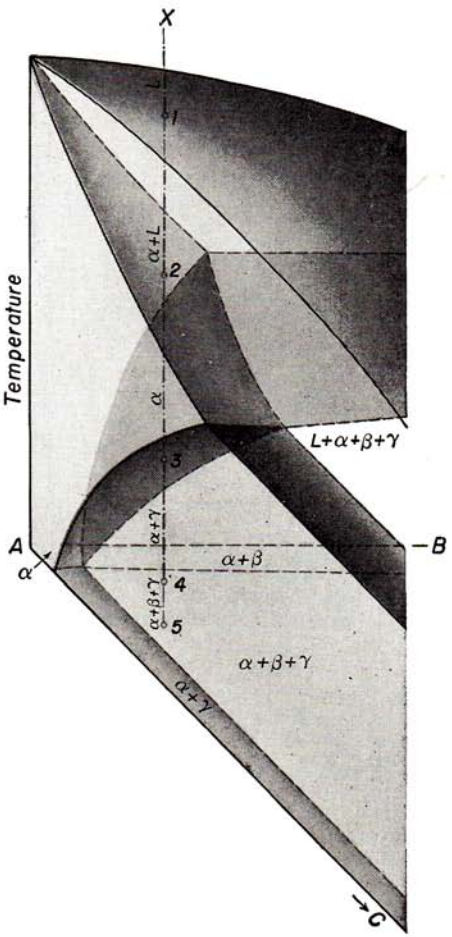

FIG. 14-11. Detail of the *A* corner of a ternary eutectic space diagram showing that a typical alloy *X* can exist in five different equilibrium states.

corresponding to the temperature of heat treatment by noting the field within which the gross composition of the alloy falls and by applying the appropriate form of the lever principle to ascertain the relative quantities of the phases that would be present at equilibrium. Since departures from the equilibrium state can be induced during freezing by coring of both

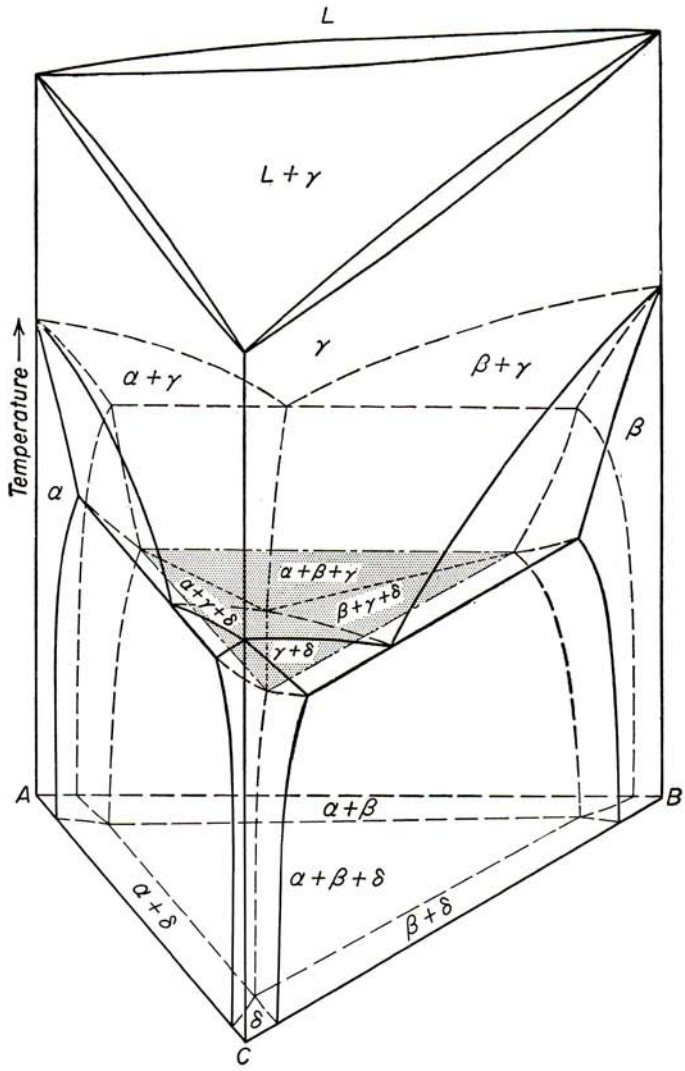

FIG. 14-12. Space diagram of an idealized ternary eutectoid system.

the primary and secondary (two-phase) constituents, and since there is also an increase in the number of changes that can be induced in the solid state by various heat-treating cycles, it is impractical to consider all possibilities here. Instead, one example involving several of the factors that are normally encountered will be discussed.

Consider an alloy of composition X, Fig. 14-11, which should be composed of $\alpha + \beta + \gamma$ at room temperature and up to temperature 4. Above

4 and up to 3, it would be composed of $\alpha + \gamma$, from 3 to 2 of α alone, from 2 to 1 of $L + \alpha$, and above 1 of liquid alone. This alloy, if normally frozen, would have a microstructure similar in kind to that of Fig. 14-8C; i.e., there would be a primary constituent of cored α, a secondary constituent of cored $\alpha + \gamma$, and a tertiary constituent composed of the ternary eutectic $\alpha + \beta + \gamma$. If held at a temperature between 2 and 3 the

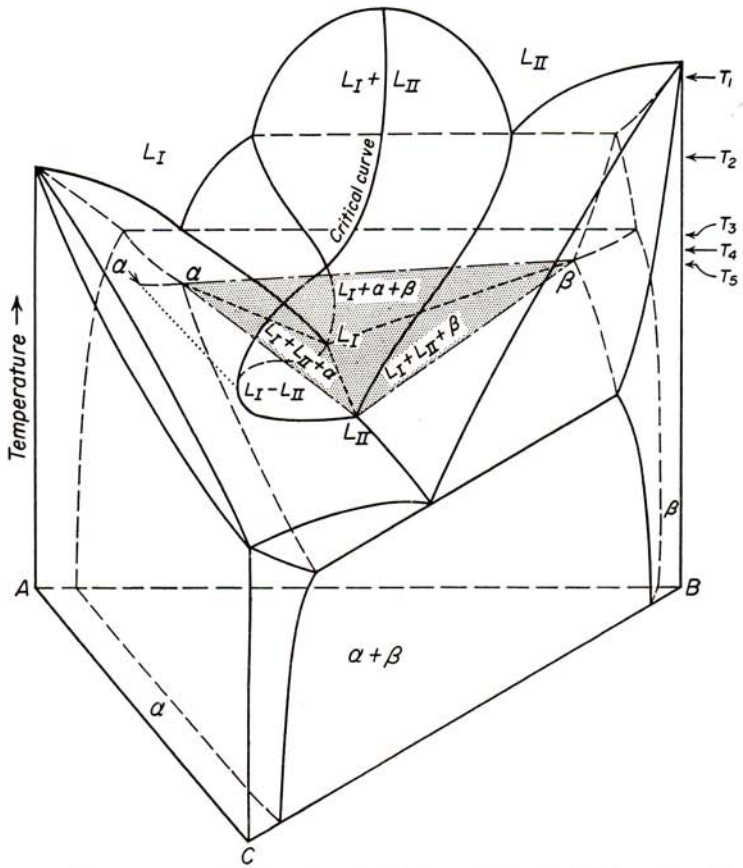

FIG. 14-13. Space diagram illustrating class I four-phase equilibrium involving two immiscible liquid phases.

β and γ phases would dissolve completely in the α, coring of the α phase would be reduced, and the alloy, if quickly cooled from this temperature and examined, would be found to be composed of homogeneous α and no other phase. Subsequent reheating to a temperature between 3 and 4 would cause a Widmanstätten precipitate of γ to form, or reheating to a temperature below 4 would cause both β and γ to precipitate in Widmanstätten array. This might or might not be accompanied by age-

hardening effects, depending upon whether or not the conditions described in Chap. 4 are met.

If, instead of heating the cast alloy at a temperature between 2 and 3, it is held at a temperature between 3 and 4, only the β phase will be dissolved. The γ phase, which is present in lesser quantity, would, in all probability, become spheroidized so that if quenched, the heat-treated

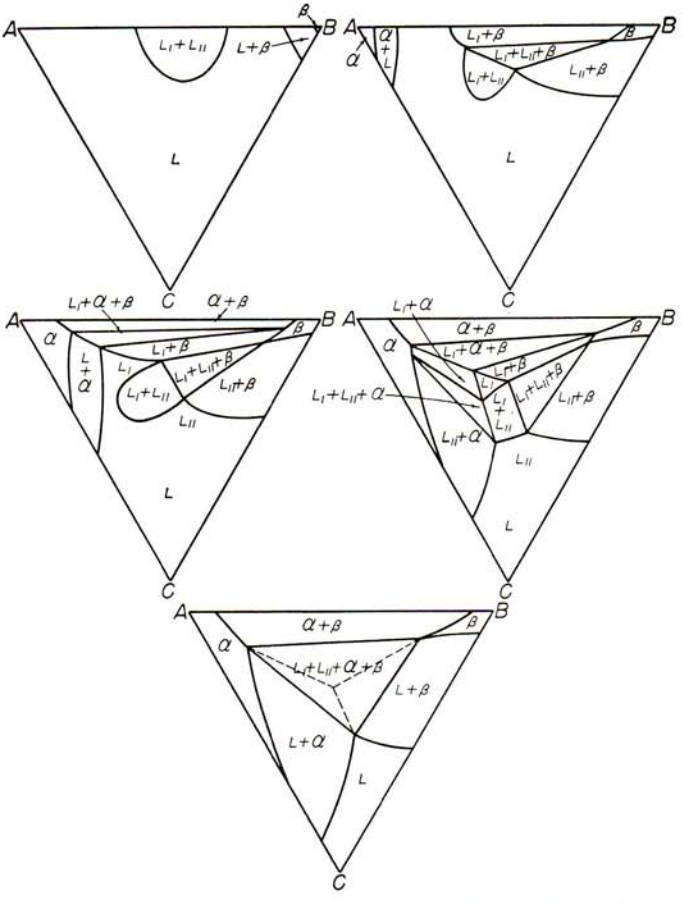

FIG. 14-14. Isotherms through the space diagram of Fig. 14-13.

alloy would be found to be made up of a matrix of homogeneous α surrounding rounded particles of γ. Reheating below temperature 4 would cause the appearance of a Widmanstätten precipitate of β.

Liquation of this alloy can also appear in several different ways. If the alloy is previously homogenized in the α field, liquation will begin upon exceeding temperature 2. If, on the other hand, the alloy were homoge-

nized within the $\alpha + \gamma$ field, liquation would begin at some lower temperature corresponding to the bottom surface of the $L + \alpha + \gamma$ field. The as-cast alloy containing a residue of the ternary eutectic constituent will, of course, liquate at the ternary eutectic temperature unless the rate of heating is sufficiently slow to permit the β phase to be dissolved before the eutectic temperature is reached.

The Ternary Eutectoid and Some Other Examples of Class I Reactions

By substituting a solid phase for the liquid phase of the ternary eutectic, the *ternary eutectoid* is obtained (Fig. 14-12). The analogy between the relationship of the binary eutectic to the ternary eutectic and that of the binary eutectoid to the ternary eutectoid appears good in all respects. Relatively little is known, however, concerning the mechanism and rate of any ternary eutectoid transformation.

Many other reactions of the class I type are obtainable by combining other phases in this kind of diagrammatic construction. A list of all conceivable combinations of phases in class I reaction is given in Table 4, Chap. 18; only a few of these have actually been observed. A monotectic version of class I reaction is depicted in Figs. 14-13 and 14-14. Here the region of two-liquid immiscibility crosses a eutectic valley. At the intersection there are four phases L_{I}, L_{II}, α, and β, establishing isothermal equilibrium. Three three-phase regions descend from higher temperature toward the four-phase reaction plane; these are $L_{\text{I}} + L_{\text{II}} + \beta$, which originates upon the binary monotectic isotherm; $L_{\text{I}} + \alpha + \beta$, which originates upon the AB binary eutectic isotherm; and $L_{\text{I}} + L_{\text{II}} + \alpha$, which originates upon the critical tie-line αL_{I}-L_{II} (dotted in Fig. 14-13) that marks the limit of two-liquid immiscibility, as in the example of Fig. 13-26. Four-phase reaction results in the disappearance of one of the liquid phases, and below this temperature only three phases—L_{II}, α, and β—exist. Below the temperature of the BC binary eutectic only the solid phases α and β remain.

PRACTICE PROBLEMS

1. In a certain ternary eutectic equilibrium the compositions of the conjugate solid phases are $\alpha = 60\%\ A + 20\%\ B + 20\%\ C$, $\beta = 20\%\ A + 70\%\ B + 10\%\ C$, and $\gamma = 10\%\ A + 30\%\ B + 60\%\ C$. Ascertain by graphical means which of the following are possible compositions of the liquid phase of this ternary eutectic: (*a*) $50\%\ A + 20\%\ B + 30\%\ C$, (*b*) $40\%\ A + 40\%\ B + 20\%\ C$, (*c*) $20\%\ A + 60\%\ B + 20\%\ C$, (*d*) $10\%\ A + 40\%\ B + 50\%\ C$. What would be the percentages of α, β, and γ into which each "possible" liquid would separate during eutectic decomposition?

2. The ternary eutectic system ABC is associated with three binary systems of the peritectic type. Draw the space diagram, and develop isotherms sufficient in number to display the internal structure of the diagram.

3. With reference to the space diagram of Fig. 14-1, draw isopleths of constant B content at 0, 10, 20, 30, 40, 50, and 90% B.

4. Deduce the changes that should occur and the microstructure that should result from the cooling of the following alloys of the ternary eutectoid system illustrated in Fig. 14-12 from the temperature range in which only the γ phase is present down to ordinary temperature: (*a*) the ternary eutectoid alloy, (*b*) gross composition selected at random within the range of the ternary eutectoid triangle, (*c*) gross composition somewhere upon the valley leading from the CB eutectoid to the ternary eutectoid point, (*d*) gross composition somewhere upon that line in the ternary eutectoid plane connecting β with γ.

5. Deduce the course of freezing and the resulting microstructure of an alloy composed of equal parts of A, B, and C in the ternary monotectic system of Fig. 14-13.